PCIM Europe Digital Days 2020

Integrated Simulation Approach to Loss Calculations of Power Converter Systems

N. Djekanovic, M.Luo, and D. Dujic

POWER ELECTRONICS LABORATORY
ÉCOLE POLYTECHNIQUE FÉDÉRALE DE LAUSANNE

Integrated Simulation Approach to Loss Calculations of Power Converter Systems

Nikolina Djekanovic[1], Min Luo[2], Drazen Dujic[1]

[1] Power Electronics Laboratory, École Polytechnique Fédérale de Lausanne, Switzerland
[2] Plexim GmbH, Switzerland

Corresponding author: Nikolina Djekanovic, nikolina.djekanovic@epfl.ch

The Power Point Presentation will be made available after the conference.

Abstract

There is a strong need in the power electronics community to have design tools capable of performing simultaneous simulations in different domains, e.g. electric, magnetic, dielectric and thermal. Therefore, this paper presents an approach to the calculation of both semiconductor and magnetic core losses in a common simulation environment. The model of a magnetic component, such as transformer, is chosen to be permeance-based and rests on hysteresis modeling. The simulated circuit combines a full-bridge LLC resonant converter, whose transformer is based on electrical and core specifications of a $100\,\mathrm{kW}$, $10\,\mathrm{kHz}$ already realized medium frequency transformer prototype. The paper demonstrates that solely with information about the geometry, used material and electrical ratings of the transformer, it is possible to accurately estimate its core losses, allowing for their inclusion into system level simulations.

1 Introduction

In order to decrease the invested time and increase the cost efficiency when designing power converter systems, the design process is heavily relying and depending on simulations. Thereby, it is important to combine and simulate all the existing domains of a power converter system, such as electric, magnetic, dielectric and thermal, with the aim of obtaining as accurate system representation as possible. In line with this, precise and physically intuitive dynamic models of essential parts of converter systems, such as magnetic components and switching devices, are highly desired. Consequently, power electronics engineers are able to estimate losses and system efficiency in various operating points already during the design phase. So far, detailed models of semiconductor power devices, such as IGBTs, MOSFETs and diodes have been developed and implemented in analog electronic circuit simulation tools, such as many versions of the computer software SPICE (ISPICE, LTspice, PSPICE) [1]–[3]. Similarly, in order to model magnetic components, various models of magnetic materials, specifically based on nonlinear hysteresis characterization, have been developed and integrated into magnetic component models. Some of these include the Chan-Vladimirescu model [4], the Jiles-Atherton model [5], [6] and the Preisach model [7]. The aforementioned models have been implemented in many finite element analysis tools or system-level simulation softwares of electrical circuits, for instance, ANSYS Simplorer, PSIM, PLECS, Gecko. These software packages target longer simulation times and are directed at observing general behavior of components within a power converter system. At the same time, software packages similar to SPICE focus on a shorter time frame with the aim of modeling the exact working principle of a single power device. Semiconductor manufacturers generally provide standardized data sheets, which contain numerous technical information such as maximum rated values, allowed temperatures and switching characteristics. This, as a consequence, allows the power electronic designers to estimate and know the component's behavior to a fairly reliable degree without having to test the device individually. Moreover, present circuit simulation tools use the available information within the

ISBN 978-3-8007-5245-4

data sheets in order to estimate components' losses and thermal behaviors inside a larger power converter system. However, in the case of standardized magnetic components (filter inductors, transformers), their data sheets provide ratings of the design at hand, but they are mostly sparse when it comes to providing information about the expected losses or general understanding of the design rules behind a particular component. Fortunately, there are more detailed data sheets available for magnetic core materials, containing core-loss dependency graphs, which can be used to estimate the corresponding losses. However, this data is not standardized among different vendors. The provided dependency curves were mostly obtained for sinusoidal type of excitation, which does not apply to e.g. a medium frequency transformer (MFT) operated within a power electronic converter. Furthermore, depending on the exact application, cores for magnetic components can be produced in various shapes, which was shown to have a direct impact on the magnetic losses [8].

This paper demonstrates that solely by knowing the geometry of a certain magnetic component, together with its electrical and material properties, it is possible to reliably calculate losses with the help of simulations, using recently developed magnetic models [9]. By doing so, the overall efficiency of a power converter system can be estimated (including semiconductor, core and winding losses), considering various operating points and prior to assembling the converter itself. The modeling of winding losses is not explicitly included in this paper, due to space restrictions. For verification purposes, an MFT prototype developed in [10] and introduced in Section 2 is modeled in a simulation environment with the help of an idealized model and a magnetic hysteresis models established in [9], [11]. The hysteresis model is based on the permeance-capacitance analogy (Section 4.2) and employed with the help of the Preisach model. The core losses obtained in this way are further compared to analytically calculated losses, which were acquired with an improved version of the Steinmetz equation already during the design phase of the MFT prototype [12], [13]. Finally, the work presented in the paper brings together component's design and realization by introducing an integrated approach for estimating different types of losses that a power converter system experiences in various operating points. Last but not least, it provides a connection between the electrical and the magnetic domain in a unique time domain simulation.

2 Problem Description

Resonant converter topologies are being increasingly used for various applications, mostly due to their soft switching capabilities, which provide increased efficiency [14]. Numerous topologies have been derived depending on the number and arrangement of components within the resonant tank. For simulation purposes, an LLC resonant converter was set as a topology of choice for a power converter system. Fig. 1 shows the electrical scheme of the converter comprising two full-bridge power stages, along with the MFT having the resonant capacitors mounted on it. The second stage is thereby used as a diode rectifier, since the power is transferred in a single direction. As mentioned in the Introduction, the transformer model is based on electrical and core specifications of a $100\,\mathrm{kW}$, $10\,\mathrm{kHz}$ MFT prototype, which is realized in [10] and can be seen in the same figure. Thereby, the transformer core was assembled from 48 U-shape magnetic cores, made of ferrite material $CF139$ and produced by Cosmo Ferrites Limited [15]. The used material is an equivalent version of the ferrite N87, produced by e.g. TDK [16]. The primary and secondary winding each consist of eight turns. The primary voltage is supplied with a $750\,\mathrm{V}$ DC-link. Electrical specifications of the transformer prototype are

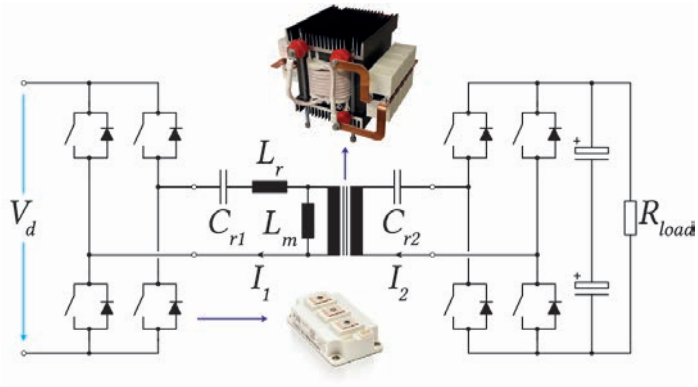

Fig. 1: Electrical scheme of the circuit, with a graphical preview of the actual components used in the experimental part.

Tab. 1: Electrical specifications of the MFT prototype developed in [10].

Electric Property	Label	Unit	Value
Rated Power	P_n	[kW]	100
Primary Voltage	V_1	[V]	$\pm$750
Secondary Voltage	V_2	[V]	$\pm$750
Switching Frequency	f_sw	[kHz]	10
Leakage Inductance	L_r	[µH]	8.4
Magn. Inductance	L_m	[µH]	750
Resonant Capacitor[1]	C_r	[µF]	18.75

summarized in Tab. 1. The load R_load is thereby gradually adjusted in order to provide loading conditions in range from 0% to 100% of the rated power. Analytically obtained core losses explained in more detail in Section 4.1.1 were determined in the design phase which eventually yielded specifications given in Tab. 1. For simulation purposes, the transformer prototype is modeled in two ways. Initially, it was presented by an idealized model (lossless and perfectly coupled) with set values of magnetizing and leakage inductance, and it was subsequently replaced by a model based on magnetic hysteresis modeling, which is explained in more detail in Section 4.2. The circuit simulation tool chosen to conduct the work is PLECS[2].

3 Semiconductor Losses

Converter losses are mainly split between the switching losses (turn-ON, turn-OFF, and diode reverse recovery losses) and the conduction losses of semiconductor power devices. Equations (1) - (5) can be used to calculate the aforenamed losses, when IGBTs and diodes are employed as semiconductor components. For certain switching instances, the corresponding data sheets provide curves with switching energies ($E_\mathrm{on}, E_\mathrm{off}, E_\mathrm{rec}$). In order to obtain additional points for the calculations an interpolation method (p^i) is used. The parameter

$$P_\mathrm{igbt,on} = \sum \frac{p^i(E_\mathrm{on}, i_\mathrm{igbt}) \cdot u_\mathrm{igbt,on}}{V_\mathrm{CC} T_\mathrm{sw}} \quad (1)$$

$$P_\mathrm{igbt,off} = \sum \frac{p^i(E_\mathrm{off}, i_\mathrm{igbt}) \cdot u_\mathrm{igbt,off}}{V_\mathrm{CC} T_\mathrm{sw}} \quad (2)$$

$$P_\mathrm{diode,rr} = \sum \frac{p^i(E_\mathrm{rec}, i_\mathrm{diode}) \cdot v_\mathrm{diode}}{V_\mathrm{CC} T_\mathrm{sw}} \quad (3)$$

$$P_\mathrm{igbt,cond} = I_\mathrm{igbt,avg} V_\mathrm{CE} + I^2_\mathrm{igbt,rms} R_\mathrm{igbt,on} \quad (4)$$

$$P_\mathrm{diode,cond} = I_\mathrm{diode,avg} V_F + I^2_\mathrm{diode,rms} R_\mathrm{d,on} \quad (5)$$

V_CC stands for the measured V_CE voltage, when the switching energy dependencies $E_\mathrm{on/off}(i_\mathrm{igbt})$, $E_\mathrm{rec}(i_\mathrm{diode})$ were being acquired, whereas T_sw is the time period over which the losses are computed. However, considering the nature of an LLC converter, no reverse recovery losses are expected. Furthermore, due to the soft switching characteristic of such converters, the same statement holds for the turn-on losses of the chosen switching devices. Nevertheless, the presented theory in this section is well known and easily integrated into a simulation environment, due to availability of standardized data sheets. Semiconductor losses obtained in the simulation with an ideal model and with a magnetic hysteresis model of the MFT are compared in Section 5.

4 Medium Frequency Transformer Modeling and Losses

The core and winding losses are principally two main contributors of total MFT losses. Hence, their accurate estimation is of high importance during the transformer's design phase. Moreover, the ability to simulate various operating points and extract losses is essential for verification of the interaction between the MFT and the surrounding power electronics. This further contributes to estimation of the overall performance and the efficiency of the converter.

4.1 Core Losses

There are various ways to estimate magnetic core losses, ranging from employing a calorimetric setup and measuring the losses directly on an existing prototype to using loss separation methods or explicit analytical equations. The approach selected in this work relies on magnetic modeling of core segments through material hysteresis modeling,

[1] The resonant capacitor bank was realized as a series connection of multiple parallel AC film capacitors accounting to 37.5µF, placed on each side of the MFT.

[2] PLECS is a registered trademark of Plexim GmbH.

whereas the analytical approach based on the Steinmetz equation was used to verify the obtained losses. In general, core losses can be divided into three parts as stated in [17]: frequency-independent hysteresis loss, frequency-dependent eddy current loss and relaxation loss. Furthermore, eddy current losses can be neglected for ferrite materials in the frequency range $\leq 50\,\mathrm{kHz}$, because of their low electrical conductivity [11]. Relaxation losses are mostly visible for high-frequency (e.g. above $20\,\mathrm{kHz}$) applications and certain voltage waveforms applied to the magnetic structure [18]. Therefore, it is assumed that the hysteresis effect generally dominates the core losses for this specific transformer case.

4.1.1 Analytical Approach

Average core power loss expressed per unit of volume can be estimated using the following well-known power density equation

$$P_\mathrm{c} = K f_\mathrm{sw}^\alpha B_\mathrm{m}^\beta, \tag{6}$$

also known as the original Steinmetz equation. Parameters K, α and β are the Steinmetz loss coefficients, f_sw is the excitation frequency and B_m is the amplitude of the magnetic flux density. Note that the Steinmetz coefficients are only valid for a limited flux density and frequency range. The coefficients can be determined based on the core loss dependency graphs ($P_\mathrm{c}(B_\mathrm{m}), P_\mathrm{c}(f_\mathrm{sw})$) expressed in logarithmic scales and provided by core manufacturers. According to (6), it is evident that losses follow a power function in both parameters f_sw and B_m. Consequently, the parameters α and β represent the slopes of the curves given in the graphs $P_\mathrm{c}(f_\mathrm{sw})$ and $P_\mathrm{c}(B_\mathrm{m})$, respectively. Once the two parameters are known, the last coefficient K can be determined from one of the points from the graphs. However, it is worth noting the inevitable uncertainty in reading data from the graphs, which arises due to limited resolution of the presented measurements. Furthermore, the aforementioned loss dependency graphs are usually provided based on sinusoidal excitation of the material. Luckily, there are analytical solutions available which enable core loss calculation for arbitrary forms of excitation. The improved generalized Steinmetz equation (IGSE) builds on the original equation in (6) and it offers the possibility to extend the estimation of core losses to any non-sinusoidal excitation waveform. From [13], the IGSE is given as

$$P_\mathrm{c} = \frac{1}{T}\int_0^T k_\mathrm{i} \left|\frac{dB(t)}{dt}\right|^\alpha (\Delta B)^{\beta-\alpha}\Delta t, \tag{7}$$

where T represents the electric period, ΔB is the peak-to-peak induction ($\Delta B = 2B_\mathrm{m}$) and the coefficient k_i is defined as following

$$k_\mathrm{i} = \frac{K}{2^{\beta+1}\pi^{\alpha-1}\left(0.2761 + \frac{1.7061}{\alpha+1.354}\right)}. \tag{8}$$

When a characteristic flux density waveform is considered, which is typical for applications involving LLC resonant converters, the IGSE expressed in (7), combined with (8) eventually yields

$$P_\mathrm{c} = 2^\beta k_\mathrm{i} f_\mathrm{sw}^\alpha B_\mathrm{m}^\beta \left[D^{1-\alpha} + (1-D)^{1-\alpha}\right], \tag{9}$$

where D stands for duty cycle. The three Steinmetz coefficients were determined as explained earlier and their values are summarized in Tab. 2. As given

Tab. 2: Steinmetz loss coefficients estimated for the investigated core material.

Parameter	K	α	β
Value	33	1.25	2.6

in Tab. 1 the excitation frequency f_sw is set to $10\,\mathrm{kHz}$ and the duty cycle to 0.5. The flux density amplitude B_m is set to $0.21\,\mathrm{T}$ and the value is directly obtained from the measured hysteresis loop of the MFT core material. Eventually, the core losses obtained with IGSE are estimated to be around $225\,\mathrm{W}$.

4.2 Magnetic Hysteresis Modeling

The magnetic model of the transformer core that was used to obtain core losses through simulation has been incorporated from the work conducted in [19]. There, a so called permeance-capacitance analogy was used, where core segments are represented by permeances, as given in the following relation

$$\mathscr{P} = \mu\frac{A}{l}, \tag{10}$$

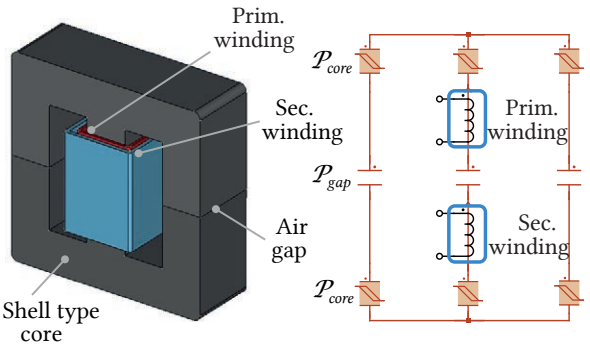

Fig. 2: Transformer core represented by a combination of permeances in a magnetic circuit. Figure is adopted from [19].

which are further combined in a magnetic circuit. The parameters A and l are related to the geometry of a certain core segment and correspond to the cross section and the magnetic path length, respectively. The material-related property μ stands for permeability and it describes the non-linear magnetic nature of the core, i.e. hysteresis. Thereby, the mathematical model of hysteresis by Preisach [7] is used and the permeability μ is modeled as a function of the magnetic field strength ($\mu(H)$). The exact modeling of the transformer core with the help of permeances (for core and air segments), which are combined in a magnetic circuit based on the core geometry is given in Fig. 2.

In order to parametrize the magnetic model in PLECS, i.e. approximate the material permeability,

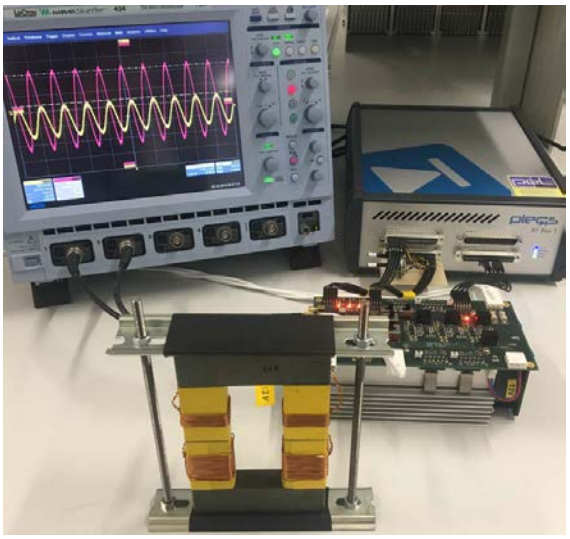

Fig. 3: Magnetic characterization setup [9] for the set of U-cores made of ferrite material CF139.

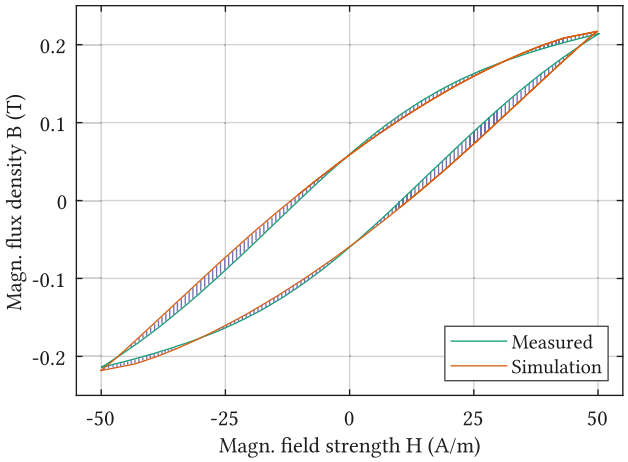

Fig. 4: Comparison of the B-H curve measured at the test setup and the simulated curve obtained with the help of the magnetic hysteresis model of the transformer core.

hysteresis measurements were taken with the help of characterization setup [9] demonstrated in Fig. 3. The primary current (excited by the power stage) and the secondary voltage are thereby measured and converted to field strength and flux density inside the control unit (PLECS RT-Box) through the following equations

$$H = \frac{N_1 \cdot I}{l} \qquad B = \frac{\int V \cdot dt}{N_2 \cdot A}. \tag{11}$$

The parameters N_1 and N_2 are numbers of turns of the primary and the secondary winding of the test core assembly. Fig. 4 shows a good matching between the measured hysteresis loop of the core material and the one obtained as a result of hysteresis modeling at no load conditions. The striped areas represent the difference between the measured and the simulated curve which results in errors of per-cycle energy. According to model verification conducted in [19] under different conditions and for variety of ferrite materials, the observed difference stays within the 10% overestimation range of the core losses at no load conditions. Furthermore, it was observed that this percentage decreases with the increase of the transferred power. With the characterized hysteresis model, the core losses of the MFT simulated as a part of the circuit presented in Fig. 1 can be taken directly from PLECS by subtraction of the power measured at the secondary side from the primary transformer side, as presented in Section 5.

ISBN 978-3-8007-5245-4

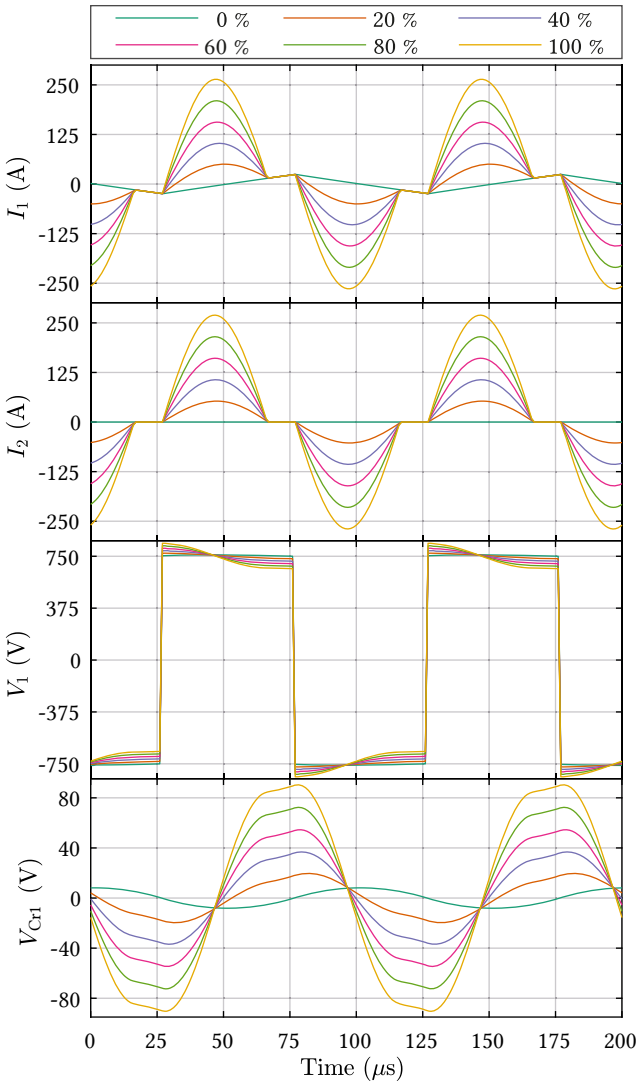

Fig. 5: Simulated current waveforms on the primary (I_1) and the secondary (I_2) MFT side, followed by the primary voltage (V_1) and the voltage acquired at the capacitor bank (V_{Cr1}) at a variable power, ranging from 0% to 100% of the rated power.

5 Simulation Results

Simulations of the circuit given in Fig. 1, for various operating points and in case the magnetic hysteresis model of the transformer is used, yielded primary and secondary current waveforms shown in the upper part of Fig. 5. The primary current at no load conditions gives the magnetizing transformer current of triangular-alike shape typical for the LLC converter (green curve labeled with 0%). The lower part of the figure shows the voltage waveforms obtained at the primary transformer side and at the capacitor bank. Furthermore, together with (1) - (4),

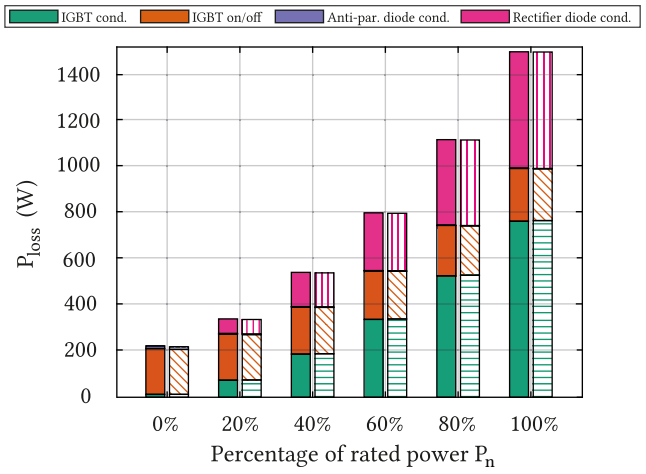

Fig. 6: Semiconductor losses calculated for various output powers with an ideal model (filled bars) and with a hysteresis MFT model (striped bars).

the waveforms are used to calculate semiconductor losses (IGBT module 5SNG 0150Q170300) of the converter. A comparison of this type of losses obtained for both transformer models is given in Fig. 6. In the left column (filled bars) the losses of the ideal model are given, whereas the right column (striped bars) represents the losses of the magnetic hysteresis model of the MFT. It can be noted that the switching losses of the IGBTs retain a similar value regardless of the output power, whereas the conduction losses of both rectifier diodes and IGBTs increase with the increase of the transferred power, which is logical taking the current increase in Fig. 5

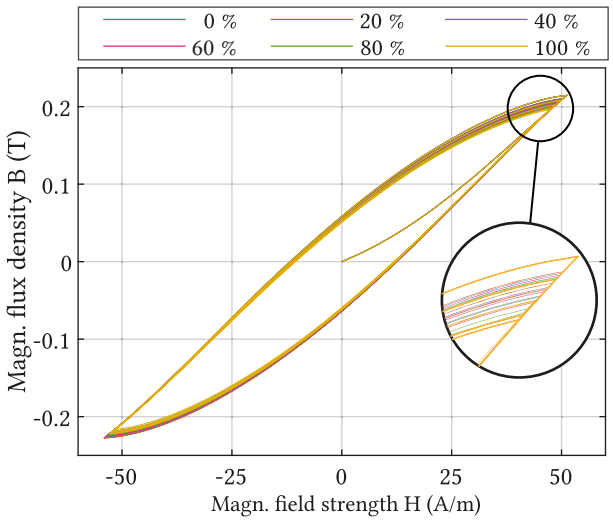

Fig. 7: Simulated B-H curves obtained with the help of the magnetic hysteresis model of the MFT at variable rated power ranging from 0% to 100%.

ISBN 978-3-8007-5245-4

Tab. 3: Core loss values acquired in simulations at variable output power.

P_n	0%	20%	40%	60%	80%	100%
$P_\mathrm{c}[W]$	229.6	226.4	223.8	221.2	218.6	216.1

into account. Eventually, it is clear from Fig. 6, that the choice of the transformer model has no effect on any of the semiconductor losses. Nevertheless, the ideal model of the transformer cannot be used to calculate the magnetic core losses, which outlines the importance of the magnetic hysteresis model.

Fig. 7 shows the hysteresis loops of the MFT core material obtained for variable transferred powers and extracted directly from the simulations. Thereby, a zoom in the upper part of the curve is provided in order to observe slight differences in descending curves for different operating points, hence, explaining the difference in overestimation for different loading conditions mentioned in Section 4.2. Tab. 3 provides an overall agreement between the losses of the transformer core, simulated with the help of the magnetic hysteresis model at variable power levels, and the analytically calculated value with the IGSE for the selected material, design and operating characteristics. The largest discrepancy between the core losses obtained through simulations and the analytically obtained value lies when the full rated power is transferred and it amounts to around 4%. In contrast to the analytical approach, determining core losses through hysteresis modeling does not directly depend on the excitation waveform. Finally, the small differences in the size of the hysteresis loops observed in Fig. 7 lead to divergence of the core loss values obtained for various loading conditions. This is recognized as an artifact of the magnetic model, which responds to slightly different voltage excitation waveforms with slightly altered hysteresis loops. The variation of the excitation depending on the operating point is visible in the primary transformer voltage presented in Fig. 5.

6 Conclusion

This paper proposes an integrated approach to loss calculation of a converter system, which includes semiconductor and magnetic core losses. Analytically obtained core losses and the losses acquired through a simulation based on a hysteresis model of a transformer match to a great extent.

Furthermore, it was shown that the electrical behavior of the transformer remains the same regardless of the model used in the simulation. This further implies that semiconductor losses remain the same regardless which of the two transformer models is used. The slight difference in the measured and the simulated curve was characterized and its effect on the core loss calculation was estimated to a maximum of 10%, leading to overestimation of the expected core losses. This could be further considered as a safe margin from the designer's point of view, but it is also a subject of ongoing research in order to improve the fidelity of the model, together with inclusion of the winding losses.

Acknowledgment

The results presented in this paper are a part of the EMPOWER project that has received funding from the European Research Council (ERC) under the European Union's Horizon 2020 research and innovation programme (Grant agreement No. 818706).

References

[1] A. R. Hefner, "A dynamic electro-thermal model for the IGBT", *IEEE Transactions on Industry Applications*, vol. 30, no. 2, pp. 394–405, 1994.

[2] C. L. Ma and P. O. Lauritzen, "A simple power diode model with forward and reverse recovery", in *PESC'91 Record 22nd Annual IEEE Power Electronics Specialists Conference*, IEEE, 1991, pp. 411–415.

[3] A. R. Hefner and D. L. Blackburn, "Simulating the dynamic electro-thermal behavior of power electronic circuits and systems", in *[Proceedings] 1992 IEEE Workshop on Computers in Power Electronics*, IEEE, 1992, pp. 143–151.

[4] J. H. Chan, A. Vladimirescu, X.-C. Gao, P. Liebmann, and J. Valainis, “Nonlinear transformer model for circuit simulation”, *IEEE Transactions on Computer-Aided Design of Integrated Circuits and Systems*, vol. 10, no. 4, pp. 476–482, 1991.

[5] D. C. Jiles and D. L. Atherton, “Theory of ferromagnetic hysteresis”, *Journal of magnetism and magnetic materials*, vol. 61, no. 1-2, pp. 48–60, 1986.

[6] D. C. Jiles and J. Thoelke, “Theory of ferromagnetic hysteresis: determination of model parameters from experimental hysteresis loops”, *IEEE Transactions on magnetics*, vol. 25, no. 5, pp. 3928–3930, 1989.

[7] F. Preisach, “Über die magnetische Nachwirkung”, *Zeitschrift für physik*, vol. 94, no. 5-6, pp. 277–302, 1935.

[8] A. Kahveci, P. Szary, F. Herget, A. K. Putri, and K. Hameyer, “Methods for hysteresis losses determinations at non-standard ring core geometries equivalent to Epstein measurements”, *2016 6th International Electric Drives Production Conference, EDPC 2016 - Proceedings*, pp. 135–142, 2016. DOI: 10.1109/EDPC.2016.7851325.

[9] M. Luo, D. Dujic, and J. Allmeling, “Modeling Frequency Independent Hysteresis Effects of Ferrite Core Materials Using Permeance–Capacitance Analogy for System-Level Circuit Simulations”, *IEEE Transactions on Power Electronics*, vol. 33, no. 12, pp. 10 055–10 070, 2018.

[10] M. Mogorovic and D. Dujic, “100 kW, 10 kHz Medium-Frequency Transformer Design Optimization and Experimental Verification”, *IEEE Transactions on Power Electronics*, vol. 34, no. 2, pp. 1696–1708, 2018.

[11] M. Luo, D. Dujic, and J. Allmeling, “Modeling Frequency-Dependent Core Loss of Ferrite Materials Using Permeance–Capacitance Analogy for System-Level Circuit Simulations”, *IEEE Transactions on Power Electronics*, vol. 34, no. 4, pp. 3658–3676, 2018.

[12] M. Mogorovic and D. Dujic, “Thermal modeling and experimental verification of an air cooled medium frequency transformer”, in *2017 19th European Conference on Power Electronics and Applications (EPE’17 ECCE Europe)*, Ieee, 2017, P–1.

[13] K. Venkatachalam, C. R. Sullivan, T. Abdallah, and H. Tacca, “Accurate prediction of ferrite core loss with nonsinusoidal waveforms using only Steinmetz parameters”, in *2002 IEEE Workshop on Computers in Power Electronics, 2002. Proceedings.*, IEEE, 2002, pp. 36–41.

[14] M Salem, A Jusoh, N. R. N. Idris, and I. Alhamrouni, “Performance study of series resonant converter using zero voltage switching”, in *2014 IEEE Conference on Energy Conversion (CENCON)*, IEEE, 2014, pp. 96–100.

[15] *Cosmo Ferrites Limited, UU Cores Product*, https://www.cosmoferrites.com/product-detail.aspx?pid=17&psid=320.

[16] *TDK Corporation*, https://product.tdk.com/info/en/products/ferrite/index.html.

[17] J. B. Goodenough, “Summary of losses in magnetic materials”, *IEEE Transactions on magnetics*, vol. 38, no. 5, pp. 3398–3408, 2002.

[18] J. Muehlethaler, J. Biela, J. W. Kolar, and A. Ecklebe, “Improved Core-Loss Calculation for Magnetic Components Employed in Power Electronic Systems”, in *IEEE Transactions on Power Electronics*, vol. 27, 2012, pp. 964–973.

[19] M. Luo, “Dynamic Modeling of Magnetic Components for Circuit Simulation of Power Electronic Systems”, p. 195, 2018. DOI: 10.5075/epfl-thesis-8801.